S1. Supplementary Methods 1

Composite samples preparation via hot pressing

To prepare specimens for microscopy and conductivity analysis, the composite powder was placed between two brass plates (95 mm x 76 mm x 6.4 mm) and pressed in a hydraulic hot press (Model 0230C-X1, PHI-Tulip) at 18 kN with a temperature of 210°C. Copper strips of 0.4 mm thickness placed between the brass plates prior to loading were used to ensure that the thickness of the resulting composite was ~0.4 mm. To facilitate transfer of the sample from the hot press to the cold press, the brass plates were placed on a larger aluminum plate (300 mm x 150 mm x 6.4 mm) before insertion into the press. The sample was held under applied force during the entire heating cycle. Once both the upper and lower plates reached 210°C (which typically took ~1 h), the sample was held in the press for an additional 15 minutes. After that time, the aluminum plate with the brass plates on it was slid out of the hot press and moved to a cold press (Model 0230C-X1, PHI-Tulip), and allowed to cool to room temperature (~10 minutes) under 18 kN of force.

S2. Supplementary Methods 2

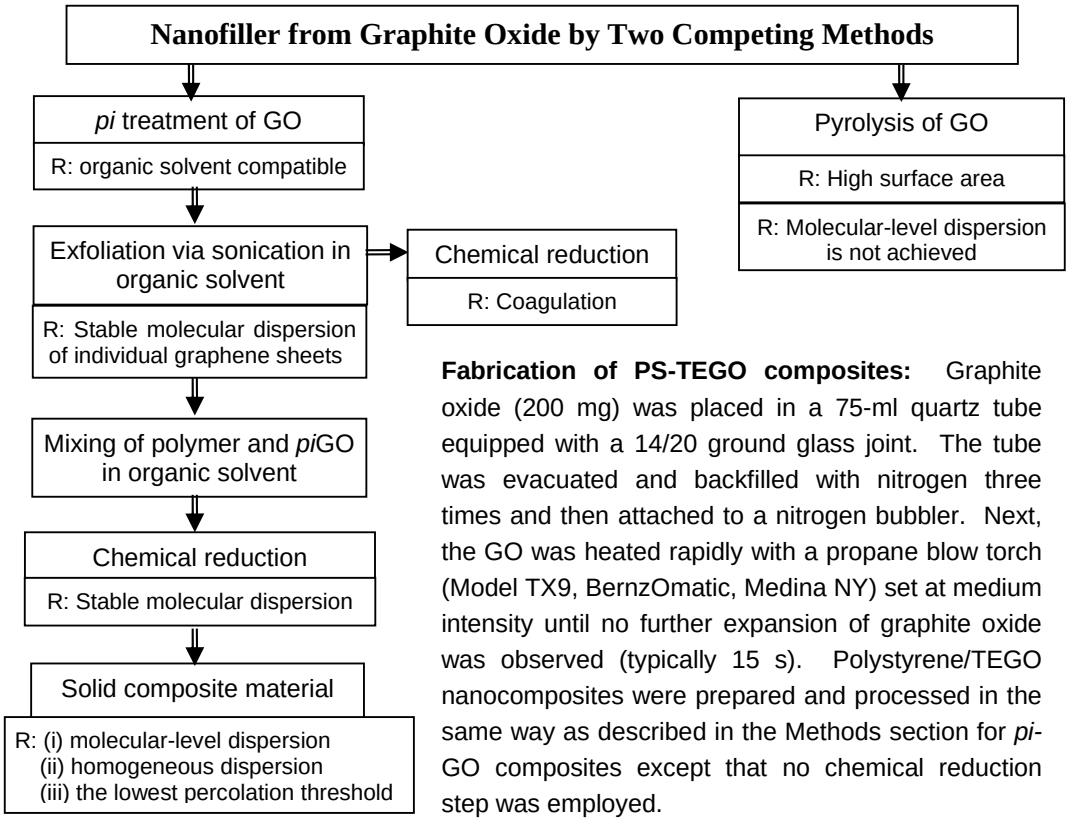

pi is acronym for phenyl isocyanate
R is acronym for *results*

Fabrication of PS-TEGO composites: Graphite oxide (200 mg) was placed in a 75-ml quartz tube equipped with a 14/20 ground glass joint. The tube was evacuated and backfilled with nitrogen three times and then attached to a nitrogen bubbler. Next, the GO was heated rapidly with a propane blow torch (Model TX9, BernzOmatic, Medina NY) set at medium intensity until no further expansion of graphite oxide was observed (typically 15 s). Polystyrene/TEGO nanocomposites were prepared and processed in the same way as described in the Methods section for *pi*-GO composites except that no chemical reduction step was employed.

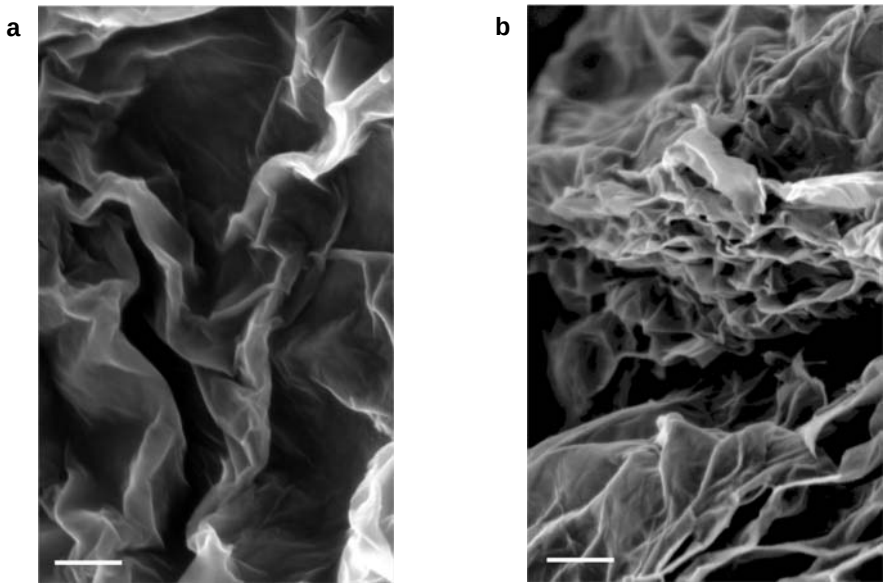

Figure S2-1. SEM images (acquired under identical conditions) of the nanofillers: **(a)** chemically reduced *pi*GO, and **(b)** thermally expanded GO (TEGO). Scale bar is 200 nm for each image.

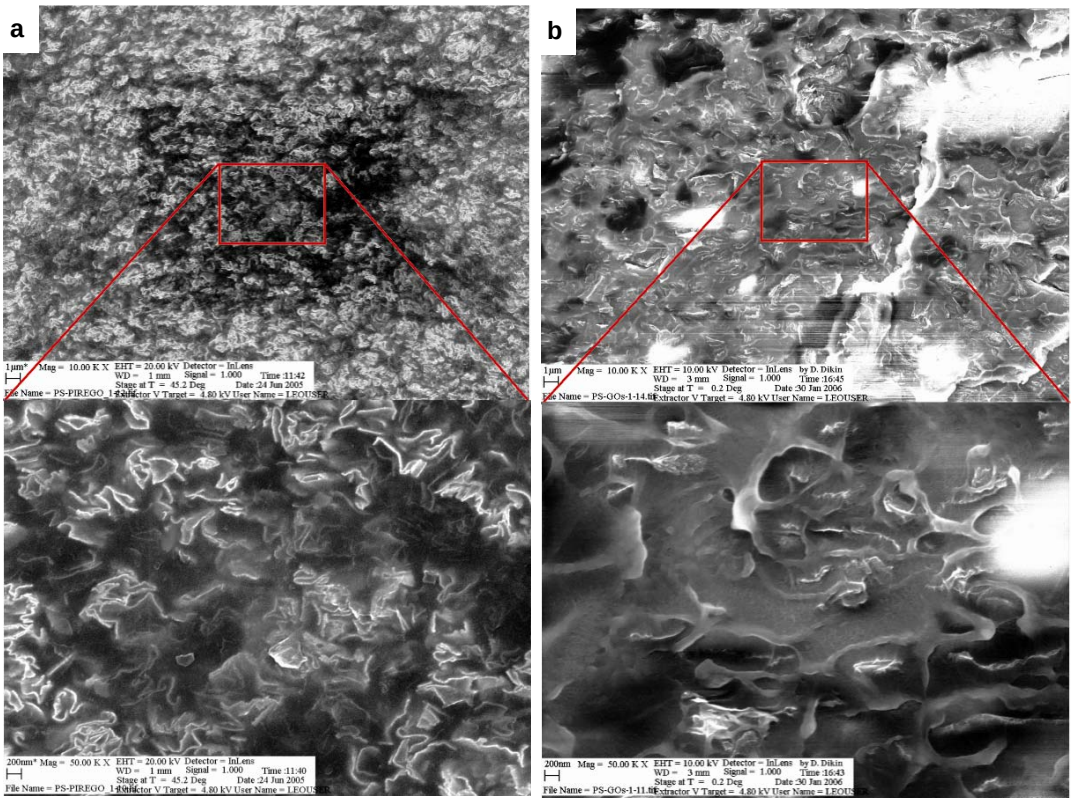

Figure S2-2. SEM images (acquired under identical conditions) of the composite fracture surfaces of the PS with 0.5 vol% dispersion of two different particle types: **(a)** Left, top and bottom. Chemically exfoliated and reduced *pi*GO, showing uniform dispersion and high particle concentration. **(b)** Right, top and bottom. Thermally expanded GO (TEGO). A much lower particle concentration of platelets and their partial agglomeration is seen in comparison to **(a)**. The heterogeneous distribution results in local charging which show up as light or dark spots.

S3. Supplementary Discussion

Explanation of electron diffraction patterns

To understand the presence of the spots with experimental d-spacing of 0.423 nm and 0.245 nm (Figure 2), we performed extensive simulation of electron diffraction patterns, using a number of approaches.

We investigated whether the diffraction patterns shown as Figures 2e inset and 2f inset of the paper were consistent with electron scatter from either graphite or from graphene layers stacked in an AA configuration. Transmission electron diffraction simulations of graphite [space group 194 / $P6_3/mmc$ with a = 0.2471 nm, c = 0.6391 nm and atoms at x = 0, y = 0, z = $1/4$ and x = $1/3$, y = $2/3$, z = $1/4$] and AA-stacked graphene [space group 187 / $P\bar{6}m2$ with a = 0.2471 nm, c = 0.6391 nm and atoms at x = $1/3$, y = $2/3$, z = 0 and x = $2/3$, y = $1/3$, z = 0] were performed using both CrystalKit / MacTempas (Total Resolution, LLC) and CrystalMaker (CrystalMaker Software, Limited) software packages. Neither graphite nor AA-stacked graphene yielded simulated diffraction spots with d-spacings of 0.426 nm and 0.245 nm. This is explained by the occurrence of destructive interference caused by the presence of "scattering" planes in both of the structures that are situated halfway between those planes separated by each of these two distances. One example of such destructive interference is shown for the case of AA-stacked graphene (Figure S3-1). Similar representations can be drawn to show the elimination of the 0.426 nm spacing in graphite, and the 0.245 nm spacings in both AA-stacked graphene and graphite.

Scattering from a single atomic layer is not amenable to simulation with the softwares that we utilized above because those packages base their simulations on calculations of the "Structure Factor", which includes within it an assumption of a three-dimensional unit cell. In the case of MacTempas – which is a 'multi-slice' algorithm[1] – it is possible to input scatter

from a single slice. Despite this, the resulting output is still dynamical in nature, and thus includes the possibility of beam interference.

We believe that the wrinkled and individual sheet morphology plays a role in the presence of the spots with experimental d-spacing of 0.423 nm and 0.245 nm, and the relative intensities of the diffraction spots observed in our materials. While simulating these observables is beyond our current simulation capability, it should present a fascinating challenge for experts having strong expertise in electron scattering.

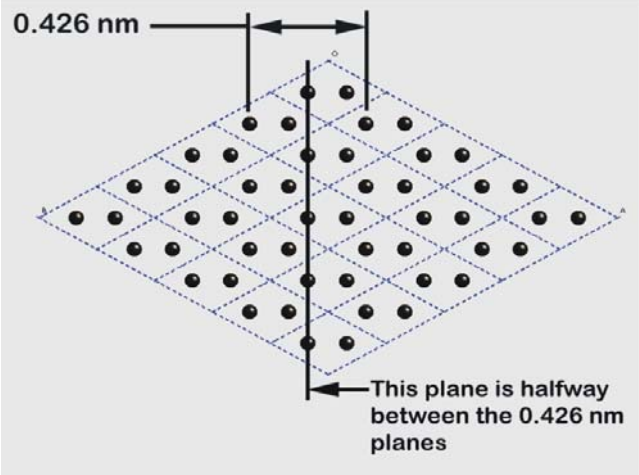

Figure S3-1 Example of destructive interference caused by scatter from a plane halfway between the $<1\bar{1}00>$-type planes spaced 0.426 nm apart.

References

1. Cowley, J. M. & Moodie, A. F. *Acta Cryst.* **10**, 609 (1957); ibid **12**, 353, 360, 367, (1959).